Proceedings of the 1997 IEEE
International Conference on Robotics and Automation
Albuquerque, New Mexico - April 1997

Intelligent Torque Sensing and Robust Torque Control of Harmonic Drive Under Free–Motion

H.D. Taghirad† and P.R. Bélanger‡
Center for Intelligent Machines,
Department of Electrical Engineering,
McGill University, Montréal, H3A 2A7
† taghirad@cim.mcgill.ca, ‡ pbelange@fgsr.lan.mcgill.ca

Abstract—

A harmonic drive is a compact, light–weight and high–ratio torque transmission device which is used in many electrically actuated robot manipulators. In many robotic control strategies it is assumed that the actuator is an ideal torque source. However, converting harmonic drive systems to ideal torque sources is still a challenging control problem for researchers. In this paper the torque control of harmonic drive system under free motion is examined in detail. A built–in torque sensor is developed in order to measure the torque, and by employing a Kalman filter the undesired torque signatures like torque ripples and misalignment torque are filtered out. An empirical nominal model for the system is obtained through experimental frequency response estimates, and the deviation of the system from the model is encapsulated by multiplicative uncertainty. A robust torque controller is subsequently designed in an $\mathcal{H}_\infty$–framework and implemented employing Kalman filtered torque estimates. From time and frequency domain experiments, it is shown that the closed–loop system retains robust stability, while improving the tracking performance exceptionally well.

I. Introduction

Robot manipulators require actuators with high torque capability at low velocities. On the contrary, DC–motors provide their operating torque only at high velocities. Many electrically actuated robots therefore, use a gear transmission to increase the torque and decrease the operating speed. Among gear transmissions, harmonic drives are high–ratio, compact and light–weight mechanisms with almost no backlash. These unique performance features of harmonic drives has captured the attention of designers. This mechanical transmission, occasionally called "strain-wave gearing", employs a continuous deflection wave along non-rigid gear, named *flexspline*. This allow for gradual engagement of gear teeth, but reduce the transmission stiffness and introduce vibration at the output shaft. This vibration appears in output speed and torque of the system, and is significant at the resonant frequency of the system [7].

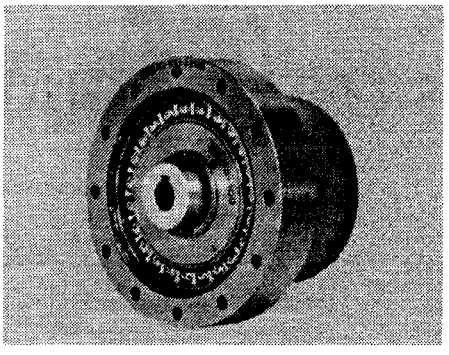

Fig. 1. Harmonic drive

In numerous robotic control techniques such as feedback linearization, computed torque method and some adaptive control schemes, actuator torque is taken to be the control input [10], [13], [12]. The physical variable being manipulated in practice, however, is not torque but armature current in a DC motor, for instance. For harmonic drive systems the relation between output torque and input current possesses nonlinear dynamics, due to the flexibility, Coulomb friction and structural damping of the harmonic drive [14]. Therefore, it is desired to improve this input/output relation by torque feedback, and to convert the system to an ideal torque source with a flat frequency response over a wide bandwidth. Brigdes et al. [1], Kaneko et al. [8], Kazerooni [9], are representative of researchers who worked on this problem. Bridges used a very simple linear model for the system, with PD torque control [1]. His results show some improvement in tracking error, but insufficient performance near resonant frequency. Kaneko also based his analysis on a simple model of the system, but included nonlinear stiffness in the system [8]. He then applied a feedforward loop to adjust for nonlinear stiffness and then a pure gain torque feedback to shape the performance. Kazerooni considers a simple linear system for the harmonic drive, and used a sensitivity loopshaping technique to design a linear controller for the system [9].

In this paper torque–control of harmonic drive system under free motion is restudied in details. First the built–in torque sensor proposed by Hashimoto et al. in 1987 [4], is developed for our harmonic drive testing station. Kalman filter estimation is proposed to estimate and filter the oscillation in the torque measurements, and the misalignment torque signature. Then an $\mathcal{H}_\infty$framework is proposed to design a robust torque controller for the system. It is shown that an empirical linear model obtained from experimen-

0-7803-3612-7-4/97 $5.00 ©1997 IEEE

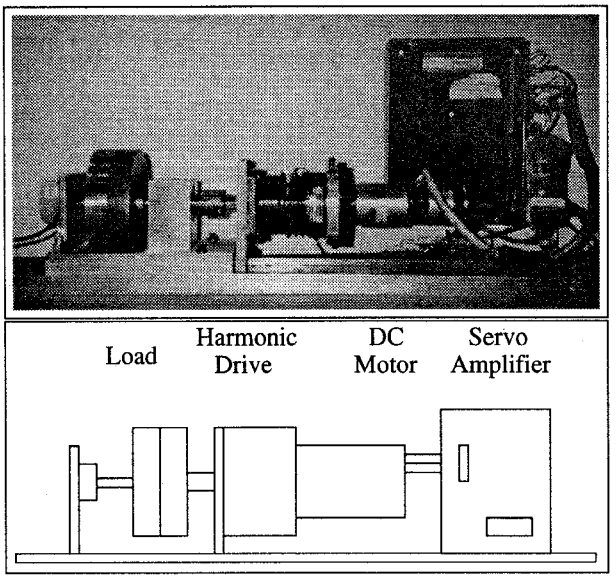

Fig. 2. Picture of the experimental setup and its schematics

tal frequency responses of the system, and an uncertainty characterisation of this model is sufficient to build a robust torque controller. Mixed–sensitivity problem is solved for the controller design, and the proposed controller is implemented and experimented. The closed–loop performance in time and frequency domains is shown to be exceptionally good.

II. Experimental Setup

A harmonic drive testing station is employed to monitor the behaviour of the system in free–motion experiments. A picture of the setup and its schematics are illustrated in Figure 2, in which the harmonic drive is driven by a DC motor, and a load inertia is used to simulate the robot arm for unrestrained motion. In this setup, a brushed DC motor from Electro–Craft is used. Its weight is 1360 grammes, with maximum rated torque of 0.15 Nm, and torque constant of 0.0543 Nm/amp. The servo amplifier is a 40 Watts Electro–Craft power amplifier. The harmonic drive is from RHS series of HD systems, with gear ratio of 100:1, and rated torque of 40 Nm.

The setup is equipped with a tachometer to measure the motor velocity, and an encoder on the load side to measure the output position. The current applied to the DC motor is measured from the servo amplifier output and the output torque is measured by a Wheatstone bridge of strain gauges mounted directly on the flexspline [4]. The details of torque sensing technique will be elaborated in Section III. These signals were processed by several data acquisition boards and monitored by a C-30 Challenger processor executing compiled computer C codes. Moreover, Siglab [3], a DSP hardware linked to Matlab, is used for frequency response analysis of the system. This hardware is capable of generating sine-sweep, random, and chirp function inputs to the system, and analyse the output signals and generate online frequency response estimates of the system.

III. Intelligent Torque Sensor

In order to apply torque feedback on the robot joint, it is necessary to measure the transmitted torque through the actuator transmission mechanism. Conventionally, torque sensor are placed in the output transmission line of the robot; however, for harmonic drive transmission which has an elastic element named flexspline, there is no advantage to add an additional compliant element and reduce the joint stiffness in order to measure the joint torque. In this paper we are using the idea of built-in torque sensor for harmonic drives as first proposed by Hashimoto and Paul in 1987 [6]. This method proved to be an economical and effective way of torque sensing for harmonic drives in our setup, as claimed by Hashimoto et al. [4], [5]. In our setup a Wheatstone bridge of four Rosset strain–gauges is utilized to sense the torsional torque transmitted through the flexspline. Rosset strain–gauge, which is an assembly of two perpendicular strain–gauges mounted on top of each other, are used to compensate for the effect of elliptical shape of the flexspline [4]. Figure 3 illustrates the strain–gauges mounted on the diaphragm part of the flexspline.

One important characteristic of harmonic drive torque transmission as observed in free motion, is a high frequency oscillation in output torque signal (See torque curve in Figure 4). These oscillation, named torque ripples, are also observed by some other researchers [2]. Torque ripples are are caused mainly by harmonic drive gear meshing vibration. Harmonic drive gear meshing vibration introduces a real torque oscillation which can be observed in the end effector motions of robots using harmonic drives and even sensed by hand when back–driving the harmonic drive. Its principal frequency of oscillation (in rad/sec) is twice the motor velocity (in rad/sec), since the gear teeth in harmonic drives are meshing in two zones. A small fraction of the torque ripples are caused by the non-ideal torque measurement, because of the direct attachment of strain gauges on the flexspline. Since the flexspline has an elliptical shape, strain gauges mounted on the flexspline are subjected to unwanted strain caused by the elliptical shape. Hashimoto [4], proposed using at least two pairs of Ros-

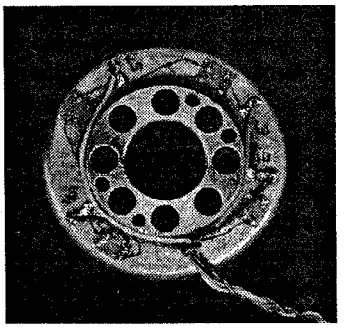

Fig. 3. Harmonic drive built–in torque sensor

set strain gauges to compensate for this unwanted strain. However, ideal compensation is possible only if there is no angular misplacement of strain gauges on the circumference of the flexspline, which is unattainable in practice. It has been found however, that using four Rosset strain–gauges, and using an accurate method to mount the strain–gauges will reduce the amplitude of the torque ripple to a minimum. Unfortunately the frequency of torque ripples (in rad/sec) introduced by the non-ideal behavior of the sensor is also twice the motor speed (in rad/sec), since the major axis of the ellipse is travelling twice as fast as the wave generator. This make it impossible to discern the true ripples caused by the gear meshing vibration from that caused by non-ideal measurement. As illustrated in Figure 4, the power spectrum of the measured torque plotted for the time interval 0.8 to 1 sec when the velocity is almost flat and about 156 rad/sec shows two peaks at 312, and 624 rad/sec. This confirms the existence of the fundamental frequency of the oscillation as twice the velocity and shows the significance of the next important first-harmonic frequency of four times the velocity.

The dependence of the frequency content of the torque ripples on the velocity makes it possible to model them as a simple harmonic oscillator, and to employ a Kalman filter to predict and filter them from the torque measurement. Practical torque controller bandwidths may not be sufficient to compensate for the torque ripples. Thus, a fast and accurate Kalman filtered torque will be used later in the torque feedback.

A fourth–order harmonic oscillator error model can characterize both the fundamental and first-harmonic frequency content of the torque ripple. This can be represented by the following discrete state space form:

$$\begin{cases} \mathbf{x}[n+1] &= \left[\begin{array}{c|c} \mathbf{\Phi}_1[n] & \mathbf{0} \\ \hline \mathbf{0} & \mathbf{\Phi}_2[n] \end{array}\right] \mathbf{x}[n] + \mathbf{w}[n] \\ y[n] &= [\,1 \;\; 0 \;\; 1 \;\; 0\,]\mathbf{x}[n] + v[n] \end{cases} \tag{1}$$

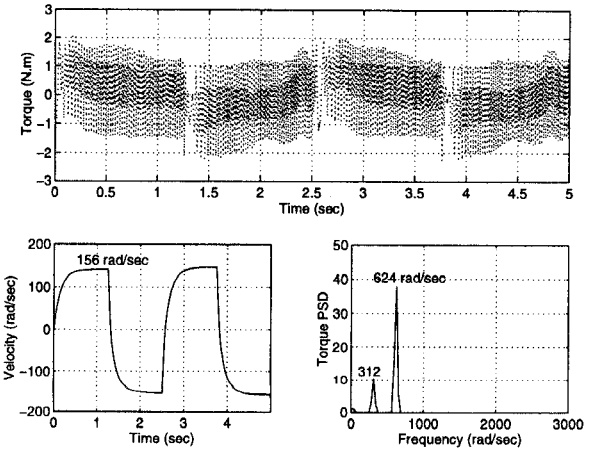

Fig. 4. Measured Torque and velocity and the power spectrum of the measured torque with peaks at multiples of the velocity

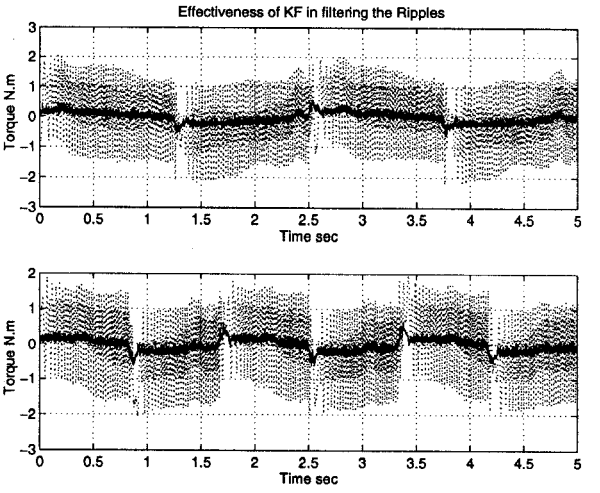

Fig. 5. Kalman filter performance to cancel torque ripples. Dotted: Measured torque, Solid: Kalman filtered torque

where

$$\mathbf{\Phi}_i[n] = \begin{bmatrix} \cos(\omega_i[n]T_s) & \sin(\omega_i[n]T_s) \\ -\sin(\omega_i[n]T_s) & \cos(\omega_i[n]T_s) \end{bmatrix} \tag{2}$$

in which T_s is the sampling period, and $\omega_1[n] = 2vel[n]$ and $\omega_2[n] = 4vel[n]$ where $vel[n]$ is the motor shaft velocity in rad/sec at time step n. Moreover, y is the torque ripple, which need to be estimated from the torque measurement by having a crude model for the expected torque. If measured torque is indicated by T_{meas}, and the expected torque is indicated by T_{exp} then torque ripple $y[n] = T_{meas}[n] - T_{exp}[n]$, while the difference between true torque and the crude expected torque is encapsulated by the measurement errors in $v[n]$ in Equation 1. For free motion experiments the expected torque can be estimated simply by the inertial part of the output torque which is the load inertia multiplied to the load acceleration. The first two elements of the state $\mathbf{x}$ consists of the component of the torque ripple due to the fundamental frequency ω_1 and its derivative, while the next two elements are those components of torque ripple due to the first-harmonic frequency ω_2, and its derivative. Therefore, the total torque ripple is calculated by adding the first and third element of the state. $\mathbf{w}[n]$ characterizes the other frequency components of the torque ripples which will not be estimated in this model.

Using the fourth–order harmonic oscillator model for the torque ripples, a prediction–type Kalman filter algorithm is applied to estimate the torque ripples [11]. A Prediction–type estimate is computationally faster than a current–estimate type of Kalman filter, and therefore preferable for online implementation. Figure 5 illustrates the performance of the Kalman filter implemented on line with a sampling frequency of 1 kHz to estimate and filter the torque ripples for two different experiments. The performance of the Kalman filter for torque ripple cancellation is shown to be quite fast and accurate.

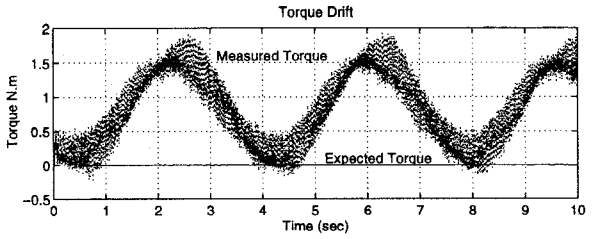

Fig. 6. Misalignment torque signature on the measured torque

The Kalman filter can be used not only to estimate the torque ripples, but also to cancel any mechanical misalignment torque signature on the measured torque. After continuous use of the harmonic drive system for different experiments for one year, a internal torque signature was observed on the measured torque which has a sinusoidal trend. Figure 6 illustrates a simple experiment in which the harmonic drive is driven by a constant velocity. The expected torque, the solid line in Figure 6, is constant after a short time of acceleration, but the measured torque, dotted lines, displays a sinusoidal behavior. After examining the system accurately, the source of this torque signature is found to be the misalignment of the harmonic drive shaft and the load. By disassembling the system and carefully reassembling it, the peak to peak amplitude of this misalignment signature was reduced from 10 N.m to less than 2 N.m. However, in practice it is quite expensive to perfectly align all the moving components. Fortunately, the sinusoidal feature of this misalignment torque makes it possible to accurately estimate them with an error model. The frequency of misalignment torque(in rad/sec), as it can be intuitively identified from its source of generation, is exactly the same as the output shaft velocity (in rad/sec). Therefore, adding another block to the harmonic oscillator model(given in Equation 1 of the system with frequency $\omega_3[n] = vel[n]/(\text{Gear Ratio})$, will estimate the misalignment component of the measured torque. Using this sixth order model for the torque ripple and misalignment torque together, Figure 7 illustrates the Kalman filter performance in cancelling those elements for two typical experiments. The Kalman filtered torque is shown to follow the expected torque trend, while cancelling the torque ripples and misalignment torque quite accurately. These results are obtained using an online Kalman filter implementation on the system with sampling frequency of 1 kHz. Although a carefully designed digital filter could cancel torque ripples with some delay, it would be incapable of extracting the misalignment torque for dynamic experiments on the system. Kalman filter estimation, on the other hand, proved to be fast, accurate and very reliable for different experiments, and therefore, used for torque feedback.

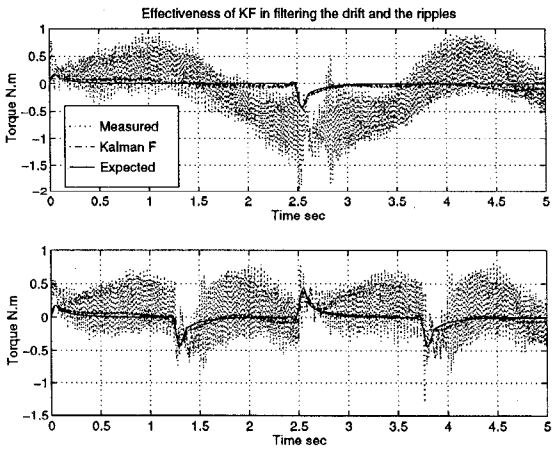

Fig. 7. Kalman filter performance to cancel torque ripples, and misalignment torque for two typical experiments

IV. Robust Torque Control

To capture the system dynamics accurately, it is necessary to consider nonlinear models for friction and structural damping [14]. However, for the purpose of control, a simple linear model for the system is sufficient for synthesis. Similar to the constrained motion case [15], an empirical nominal model for the system is derived using experimental frequency response on the system. Moreover, the frequency response variation of the system is encapsulated by multiplicative uncertainty. Figure 9 illustrates some experimental frequency responses of the system with different input amplitudes, the nominal model frequency response, and the variations in frequency response using multiplicative uncertainty.

The nominal model for the system is found to be a third order stable and minimum phase transfer function as follows:

$$\frac{\text{Torque}}{\text{Ref Voltage}} = \frac{243.16\ (s+2.415)}{s^3 + 171.19s^2 + 1.24\times 10^4 s + 1.47\times 10^5} \tag{3}$$

which has three stable poles at -14.465, and $-78.363 \pm 63.288j$. The uncertainty weighting function which is the upper bound of different uncertainty frequency plots is approximated by a second order system as:

$$\mathbf{W}(s) = \left(\frac{s+120}{145}\right)^2 \tag{4}$$

Similar to the constrained motion case [15], the control objective can be defined as *robustly stabilizing the system, while maintaining good disturbance attenuation and small*

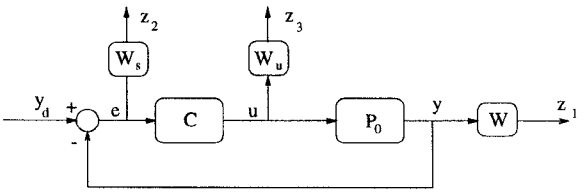

Fig. 8. Block diagram of system in $\mathcal{H}_\infty$ framework

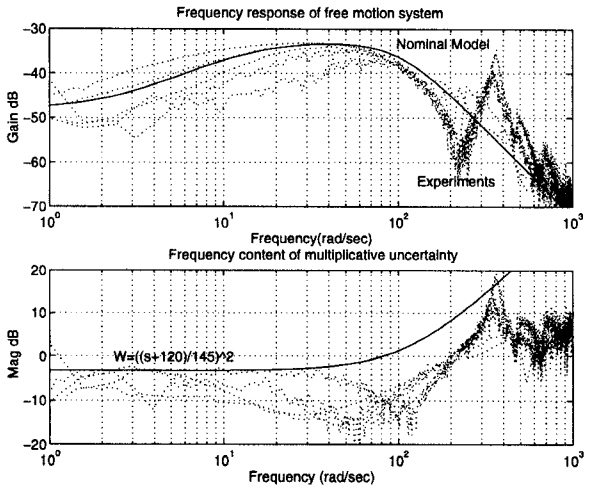

Fig. 9. Frequency response of the system, nominal model, and multiplicative uncertainty

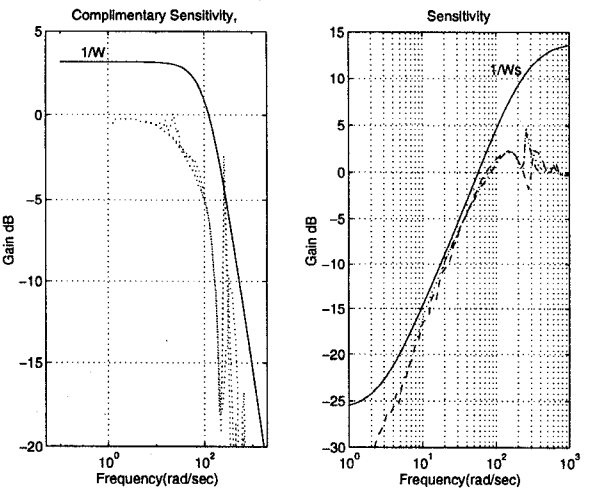

Fig. 10. Closed–loop frequency performance

tracking error, despite the actuator saturation. This objective is well–suited to the general $\mathcal{H}_\infty$problem. This control objective is translated into the general $\mathcal{H}_\infty$problem and solved using μ–synthesis toolbox of Matlab in a similar way as elaborated in the constrained motion case [15]. As illustrated in Figure 8 performance–weighting functions are selected considering the physical limitations of the system. The actuator saturation–weighting function is considered to be a constant, by which the maximum expected input amplitude never saturates the actuator. Its value is estimated to be 0.002 for free load experiments. The sensitivity–performance function is assigned to be $\mathbf{W}_s(s) = \frac{s+280}{5(s+2.8)}$. This weighing function indicates that at low frequencies, the closed–loop system should reject disturbance at the output by a factor of 20 to 1. Expressed differently, steady-state tracking errors due to step input should be less than 5 % or less.

The controller designed using μ–synthesis toolbox of Matlab has the following transfer function:

$$\mathbf{C}(s) = \frac{8.345 \times 10^5 (s+14.5)(s+78.4 \pm 63.3j)}{(s+1.83)(s+2.8)(s+273.23)(s+1.0\times 10^4)} \tag{5}$$

The controller zeros cancel the stable poles of the nominal plant, while the poles shape the closed–loop sensitivity function to lie beneath the weighting function $\mathbf{W}_s$.

V. Controller Performance

To verify the controller performance both simulations and experiments have been utilized. Here we only report the experimental results which are more convincing. To implement the controller in practice, bilinear discretization is performed with one kHz sampling frequency. The performance of the closed–loop system is evaluated in both frequency and time domain. The frequency domain performance of the closed–loop system is obtained from the closed–loop frequency response of the system and is illustrated in Figure 10. The experimental sensitivity and complementary sensitivity functions are shown to be underneath the inverse of sensitivity weighting function $\mathbf{W}_s$, and uncertainty weighting function $\mathbf{W}$ respectively. Also the Nyquist plot for the loop-gain of the system is derived from the experimental sensitivity functions, and the phase margin for the system is found to be about 80°. These results are an experimental verification of the $\mathcal{H}_\infty$design claim to preserve robust stability while shaping the performance as desired.

The time responses of the system to different reference input signals are illustrated in Figure 11. The dotted lines are the measured output torque of the system, which is tracking the solid line, the reference command, very fast and accurately. Although our designed bandwidth was about 3 rad/sec, sinusoid inputs up to 10 Hz (62 *rad/sec*) are shown to be well tracked. The step response is fast with a steady–state error less than 5 %, as required. Tracking of the system to triangular signal is especially sharp at the edges, and the tracking to an arbitrary signal is shown to be very fast and well-behaved. The main difference between harmonic drive free motion experiments and the constrained motion experiments is that in free motion case the output torque is relatively small, and therefore, the signal to noise ratio are higher than that for constrained motion case, as given in [15]. However, for both cases fast and accurate closed loop responses are obtained using $\mathcal{H}_\infty$controllers.

VI. Conclusions

In this paper the torque control of harmonic drive systems for free motion case is examined in detail. To measure the torque, a built–in torque sensor proposed by Hashimoto et al. in 1987 is employed. In this method, strain–gauges are directly mounted on the flexspline in order to not reducing the system stiffness. To cancel the torque ripples, the oscillation observed on the measured torque and caused

by gear teeth meshing, Kalman filter estimation is used. A simple forth order harmonic oscillator proved to accurately model the torque ripples. Moreover, the error model is extended to incorporate the misalignment torque signature. By on line implementation of the Kalman filter, it has been shown that this method is a fast and accurate way to filter torque ripples and misalignment torque. To design a torque controller an empirical nominal model for the system is obtained through experimental frequency response estimates using kalman filtered torques as the output of the system. It is shown that by this means there is no need to resort to a nonlinear model for the system [14]. By this method not only a nominal model for the system can be proposed, but also the deviation of the nonlinear system from the nominal model can be encapsulated in a model uncertainty. This representation provides sufficient information to build a robust torque controller for the harmonic drive system. Solving the mixed–sensitivity problem for a tracking and disturbance attenuation objective, a fourth–order $\mathcal{H}_\infty$ controller is designed respecting the actuator saturation limits. By implementing the controller, the performance of the closed–loop system is evaluated experimentally. It is shown that the closed–loop system retains robust stability, while improving the tracking performance exceptionally well.

Acknowledgements

The authors would like to express their appreciation to A. Helmy for his involvements in the experiments. Furthermore, CAE and ISE contributed the equipment used in the setup.

References

[1] M.M. Bridges, D.M. Dawson, and S.C. Martindale. Experimental study of flexible joint robots with harmonic drive gearing. *Proceedings of the IEEE Conference on Control Applications*, 2:499–504, 1993.

[2] I. Godler, K. Ohnishi, and T. Yamashita. Repetitive control to reduce speed ripple caused by strain wave gearing. *IECON Proceedings*, 2:1034–38, 1994.

[3] Signal Analysis Group. *DSP Technology Inc. Siglab Version 1.0.* DSP Technology Inc., 48500 Kato Road, Fremont, CA 94538-7385, 1994.

[4] M. Hashimoto, Y. Kiyosawa, H. Hirabayashi, and R.P. Paul. A joint torque sensing technique for robots with harmonic drives. *Proceeding of IEEE International Conference on Robotics and Automation*, 2:1034–1039, April 1991.

[5] M. Hashimoto, Y. Kiyosawa, and R.P. Paul. A torque sensing technique for robots with harmonic drives. *IEEE Transaction on Robotics and Automation*, 9(1):108–116, Feb 1993.

[6] M. Hashimoto and R.P. Paul. Integration of manipulator joint sensor information for robust robot control. *Proceeding of IEEE Conference on Decision and Control*, pages 603–604, 1987.

[7] T. Hidaka, T. Ishida, Y. Zhang, M. Sasahara, and Y. Tonika. Vibration of a strain-wave gearing in an industrial robot. *Proceedings of the 1990 International Power Transmission and Gearing Conference - New Technology Power Transmission, ASME Publications*, 1:789–794, 1990.

[8] K. Kaneko, T. Murakami, K. Ohnishi, and K. Komoriya. Torque control with nonlinear compensation for harmonic drive DC motors. *IECON Proceedings*, 2:1022–1027, 1994.

[9] H. Kazerooni. Dynamics and control of instrumented harmonic drives. *Journal of Dynamic Systems Measurement and Control - Transactions of the ASME*, 117(1):15–19, March 1995.

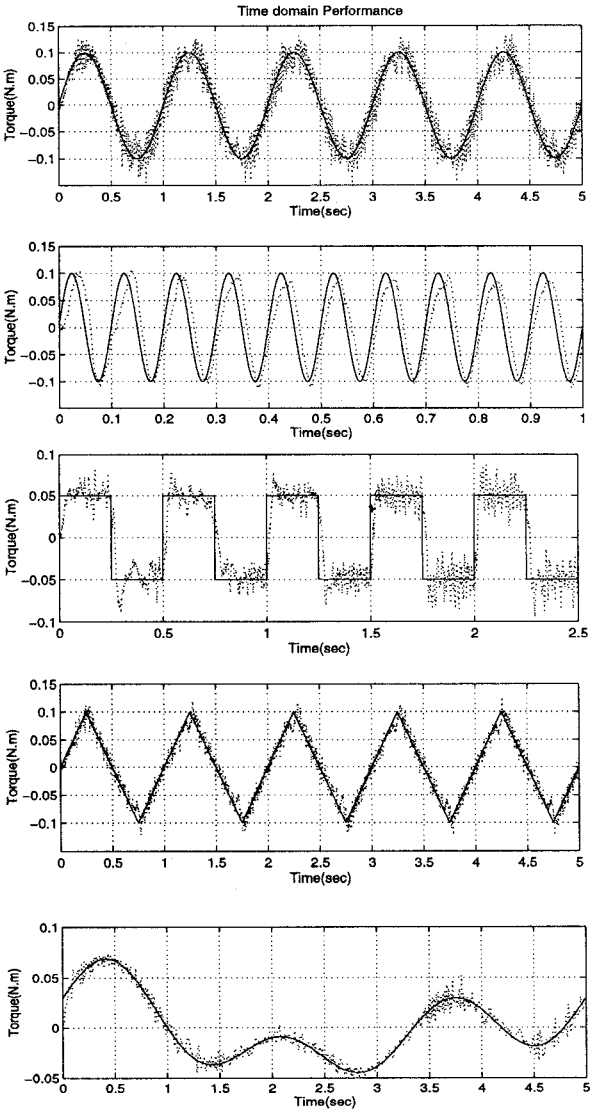

Fig. 11. Closed–loop time performance of the system employing Kalman filtered torque and robust controller

[10] S. Nicosia and P. Tomei. On the feedback linearization of robots with elastic joints. *Proceeding of IEEE Conference on Decision and Control*, 1:180–185, 1988.

[11] K. Ogata. *Discrete - time control systems.* Printice Hall, Englewood cliffs, N.J., 1995.

[12] M.W. Spong. Adaptive control of flexible joint manipulators. *Systems & Control Letters*, 13(1):15–21, Jul 1989.

[13] M.W. Spong, J.Y. Hung, S. Bortoff, and F. Ghorbel. Comparison of feedback linearization and singular perturbation techniques for the control of flexible joint robots. *Proceeding of the American Control Conference*, 1:25–30, 1989.

[14] H.D. Taghirad and P.R. Belanger. An experimental study on modelling and identification of harmonic drive systems. *In Proceedings of the 35th Conference on Decision and Control, pp 4725-30*, Dec 1996.

[15] H.D. Taghirad and P.R. Belanger. Robust torque control of harmonic drive under constrained motion. *To be presented in the 1997 IEEE International Conference on Robotics and Automation*, April 1997.